

SHORT REPORT

CDKN2A point mutations D153spl(c.457G > T) and IVS2 + 1G > T result in aberrant splice products affecting both p16^{INK4a} and p14^{ARF}Joni L Rutter¹, Alisa M Goldstein², Michael R Dávila¹, Margaret A Tucker² and Jeffery P Struewing^{*1}¹Laboratory of Population Genetics, Center for Cancer Research, National Cancer Institute, National Institutes of Health, DHHS, Bethesda, MD, USA; ²Genetic Epidemiology Branch, Division of Cancer Epidemiology and Genetics, National Cancer Institute, National Institutes of Health, DHHS, Bethesda, MD, USA

The *CDKN2A* gene, which encodes the proteins p16^{INK4a} and p14^{ARF}, is located on chromosome 9p21. Germline mutations at this locus increase susceptibility to cutaneous malignant melanoma (CMM). In general, missense and nonsense mutations are primarily responsible for defective p16^{INK4a} and possibly p14^{ARF} protein function and account for ~20% of inherited CMM cases. We report a G > T transversion mutation in the last nucleotide of exon 2, affecting the aspartic acid residue at position 153 of *CDKN2A*-p16^{INK4a} in a proband with melanoma. If splicing were unaffected, this mutation would change Asp to Tyr. RT-PCR analysis, however, revealed that this mutation, which we have termed D153spl(c.457G > T), and a previously described mutation at the next nucleotide, IVS2 + 1G > T, result in identical aberrant splicing affecting both p16^{INK4a} and p14^{ARF}. The two main alternate splice products for each of the two normal transcripts includes a 74 bp deletion in exon 2, revealing a cryptic splice site, and the complete skipping of exon 2. The dual inactivation of p16^{INK4a} and p14^{ARF} may contribute to the CMM in these families.

Oncogene (2003) 22, 4444–4448. doi:10.1038/sj.onc.1206564

Keywords: melanoma; RT-PCR; alternate reading frame; cryptic splice site

Cutaneous malignant melanoma (CMM) is the most fatal form of skin cancer and its etiology is varied and complex. Approximately 5–12% of malignant melanomas occur in individuals who have at least one first-degree relative with CMM (Goldstein and Tucker, 2001). *CDKN2A* is located on chromosome 9p21 (Kamb *et al.*, 1994; Nobori *et al.*, 1994) and mutations in this gene are present in 10–25% of melanoma-prone families (Goldstein *et al.*, 2000). The likelihood of detecting a *CDKN2A* mutation in a melanoma patient increases as the number of cases within the family increases.

*Correspondence: JP Struewing, Laboratory of Population Genetics, NCI/NIH/DHHS, Building 41, Room D702, 41 Library Drive, MSC 5060, Bethesda, MD 20892-5060, USA; E-mail: jsl40a@nih.gov
This article is a 'United States Government Work' paper as defined by the US copyright Act

Received 17 December 2002; revised 25 February 2003; accepted 5 March 2003

Mutations in the *CDKN2A* gene have been found in 50% of the families with six or more affected members, but drops to 20–40% in families with three or more affecteds, and to <5% in families with two or more CMM members (Kefford *et al.*, 1999).

CDKN2A is a complex gene that encodes two distinct proteins, p16^{INK4a} and p14^{ARF}. Despite arising from the same gene, there is no protein sequence similarity between these products (Quelle *et al.*, 1995). p16^{INK4a} is encoded by exons 1 α , 2, and 3 and functions as a cyclin-dependent kinase inhibitor of the cell cycle by inhibiting the activity of the cyclin-dependent kinase complex, CDK4/CDK6/cyclin D, thereby blocking the passage from G₁ into S by inhibiting the pRB phosphorylation (Serrano *et al.*, 1993; Rocco and Sidransky, 2001). The alternate reading frame product, p14^{ARF}, is encoded by a different first exon (exon 1 β) that is 15 kb upstream of exon 1 α , using the same second exon as p16^{INK4a} but in a different reading frame (Rocco and Sidransky, 2001). The amino-acid coding sequence of p14^{ARF} ends in exon 2, with the remainder of exon 2 and exon 3 comprising the 3'-untranslated region (reviewed in Haber, 1997). p14^{ARF} functions by preventing p53 degradation, thereby allowing p53-mediated apoptosis or cell cycle arrest (Pomerantz *et al.*, 1998).

As part of an ongoing IRB-approved genetic epidemiology study of familial melanoma (Genetic Epidemiology Branch, National Cancer Institute), probands from families with at least two living first-degree relatives with invasive melanoma are screened for mutations in the *CDKN2A* gene. In one new family (AY), we identified a mutation in the donor splice site for exon 2. The family included three patients with confirmed CMM in three generations (one child and one grandchild of the index case). Only one patient from this family was available for testing. This mutation and a previously identified (but uncharacterized) one in the next nucleotide, IVS2 + 1G > T, from family Q (Hussussian *et al.*, 1994) were analysed further to determine their effect on splicing.

Genomic DNA sequencing revealed a G > T transversion mutation in Family AY in the last nucleotide of exon 2, which is the first base of codon 153 (Figure 1). Once this mutation was identified, we also included a member from Family Q in the analysis for comparison.

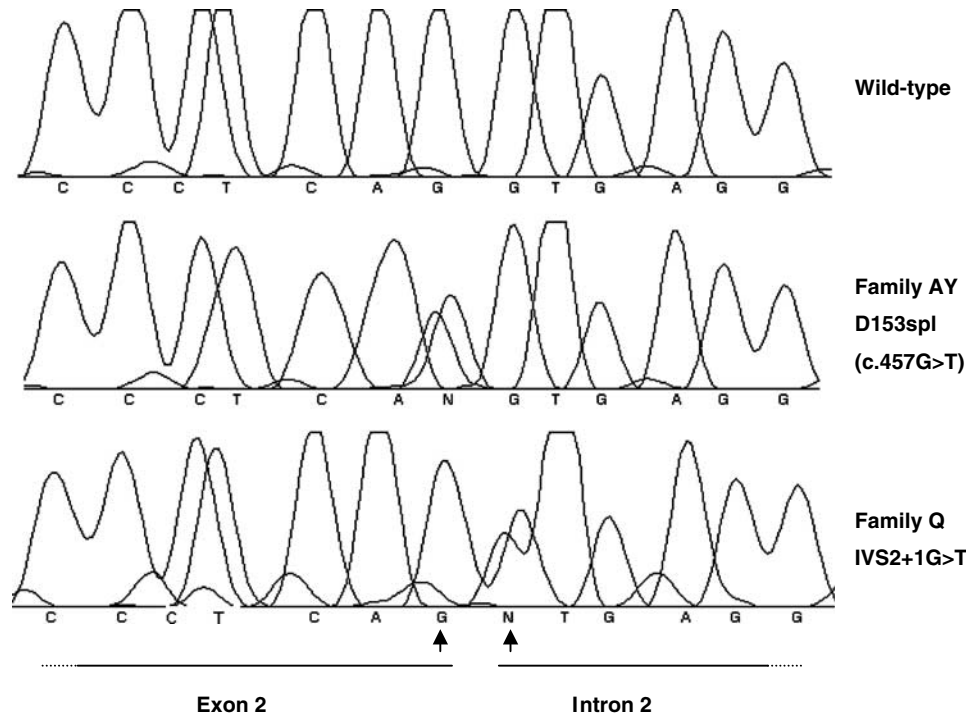


Figure 1 Sequence analysis of genomic DNA from Families AY and Q showing *CDKN2A* exon 2 and flanking sequence. The arrows indicate the heterozygous mutations. DNA and RNA were isolated from lymphocytes using the TRI REAGENT LS according to the manufacturer's instructions (MRC, Inc., Cincinnati, OH, USA). Genomic DNA was used in a PCR reaction to amplify *CDKN2A* exon 2 and flanking sequence using exon 2 forward sequencing primer: 5'-AGCTTCCTTTCCGTCATGC-3'; exon 2 reverse sequencing primer: 5'-GGAAGCTCTCAGGGTACAAATTC-3'. The PCR reaction consisted of 2 μ l 10 \times *Taq*Gold buffer, 2 μ l 25 mM MgCl₂, 1 μ l 10 mM dNTP, 200 nM each primer, 1 U *Taq*Gold Polymerase (Applied Biosystems, Foster City, CA, USA), 1.25 M betaine, and water to a final volume of 20 μ l. Cycling consisted of 94°C for 7 min, followed by 14 cycles of 95°C for 20 s, annealing at 68°C for 1 min, and extension at 72°C for 20 s, with the extension temperature being decreased 0.5°C per cycle, followed by 31 cycles of 95°C for 20 s, 61°C for 20 s, and 72°C for 20 s, followed by 72°C for 10 min. Sequencing reactions were performed using the ABI PRISM BigDye™ Terminator Cycle Sequencing Kit (Applied Biosystems, Foster City, CA, USA) and the products were analysed using an ABI 3100 Genetic Analyzer (Applied Biosystems, Foster City, CA, USA). Sequences were obtained in both the forward and reverse direction, and aligned using the VectorNTI Suite 6 software package (Informax, Inc., Rockville, MD, USA)

Family Q harbors the IVS2 + 1G>T mutation and includes two siblings with invasive melanoma, one of their parents with both melanoma and pancreatic cancer, and a grandparent with pancreatic cancer (Hussussian *et al.*, 1994; Goldstein *et al.*, 2000). All patients from this family had the IVS2 + 1G>T mutation or were obligate carriers.

On initial inspection of the DNA sequence only, the G>T mutation from family AY resembled a missense mutation, changing the aspartic acid residue at codon 153 to a tyrosine residue. Upon RT-PCR and sequencing analysis, however, a D153Y mutation was not evident. Instead, the mutation created aberrantly spliced products, thus we have termed this mutation D153spl(c.457G>T) to indicate a splice mutation in codon 153 of p16^{INK4a}, which is nucleotide 457 of p16^{INK4a} when counting from the ATG initiation codon (nucleotide 728 of the p16^{INK4a} reference mRNA sequence NM_000077.2 and nucleotide 785 of the p14^{ARF} sequence NM_058195.1). This mutation, initially thought to be novel, appears to be the same as a previously published but uncharacterized mutation called D145C (Moskaluk *et al.*, 1998).

The D153spl(c.457G>T) mutation generated similar splicing products as the previously identified intronic

mutation IVS2 + 1G>T, affecting not only p16^{INK4a}, but also p14^{ARF}. Figure 2 is a representative gel of an RT-PCR experiment with amplified products from both *CDKN2A* transcripts. The arrows indicate the similar wild-type bands and four main aberrant splice products in an individual with the IVS2 + 1G>T and the D153spl(c.457G>T) mutations. These bands were excised from the gel and sequenced. Some smaller products can be seen in the p14^{ARF}; however, these were not reproducible and sequence information either did not work or showed no similarity to *CDKN2A*. The samples with the D153spl(c.457G>T) and the IVS2 + 1G>T mutations (lanes 1, 2 and 7, 8) produced the same products, which were of lower molecular weight than the wild-type allele (lanes 3 and 9).

In normal splicing conditions, the last base of exon 2 is spliced to the first two bases of exon 3 to create the aspartic acid (GAC) at position 153 in the p16^{INK4a} protein coding sequence (indicated by the solid double-headed arrow and the solid bar over the codon sequence, Figure 3). Sequence analysis of the excised bands of splice product 1 α (Figure 2) from both the D153spl(c.457G>T) and the IVS2 + 1G>T mutations showed a deletion of 74 bp because of a cryptic splice site within exon 2. Figure 3 shows the cryptic donor

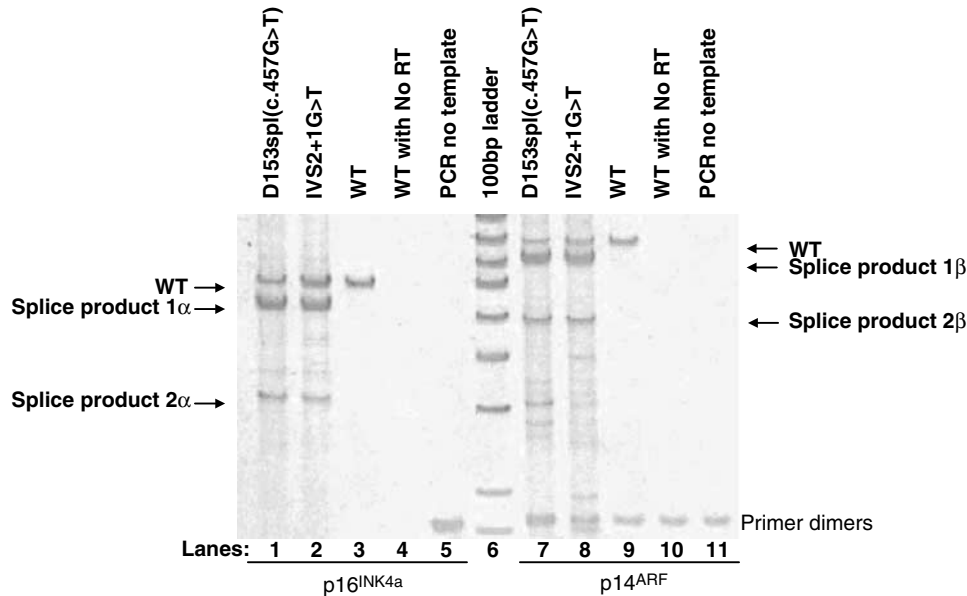


Figure 2 Representative gel showing RT-PCR products produced by the D153spl(c.457G>T) and IVS2 + 1G>T mutations. Arrows indicate specified products. p16^{INK4a} products (designated as α) are to the left of the 100 bp ladder, and p14^{ARF} products (designated as β) are on the right. The isolated RNA was resuspended in DEPC-treated water and 5 μ l were used in a reverse-transcriptase PCR assay using the ThermoScriptTM RT-PCR system (Invitrogen, Carlsbad, CA, USA). Briefly, reverse transcribed products were made using 0.5 μ l random hexamer (50 ng/ μ l), 0.5 μ l oligo (dT)₂₀ (5 μ M), 2 μ l 10 mM dNTP mix, 4 μ l 5 \times cDNA synthesis buffer, 1 μ l each of 0.1 M DTT, RNase OUTTM (40 U/ μ l), and ThermoScriptTM RT (15 U/ μ l) to a final volume of 20 μ l with water. The reaction was incubated for 10 min at 25°C, then 50 min at 55°C. Following the incubation, RNase H (1 μ l) was added to each tube and incubated for 20 min at 37°C. A measure of 1 μ l of the resultant product was used in a PCR reaction to amplify p16 and p14^{ARF} transcripts. Primers for the cDNA-specific products were as follows: p16 forward, 5'-GAGCAGCATGGAGCCTTC-3'; p16 reverse, 5'-CCTGTAG-GACCTTCGGTGAC-3'; p14^{ARF} forward, 5'-GGAATTCGAGTGGCGCTGCTCACCTC-3'; and p14^{ARF} reverse, 5'-AAAACACTAC-GAAAGCGGG-3'. The products were electrophoresed on a 1.4% agarose gel or a 6% 1 \times TBE acrylamide vertical gel (shown) and visualized using a UV transilluminator. Wild-type products and products that deviated from the expected size of the wild-type product (arrows) were excised from the gel and the DNA was isolated using the gel extraction protocol from the GENECLEAN SPIN kit (Bio101, Vista, CA, USA). Sequences were obtained using the primers listed above and the conditions described in Figure 1 (sequence traces not shown). RT-PCR and sequencing experiments were performed at least twice to confirm the findings

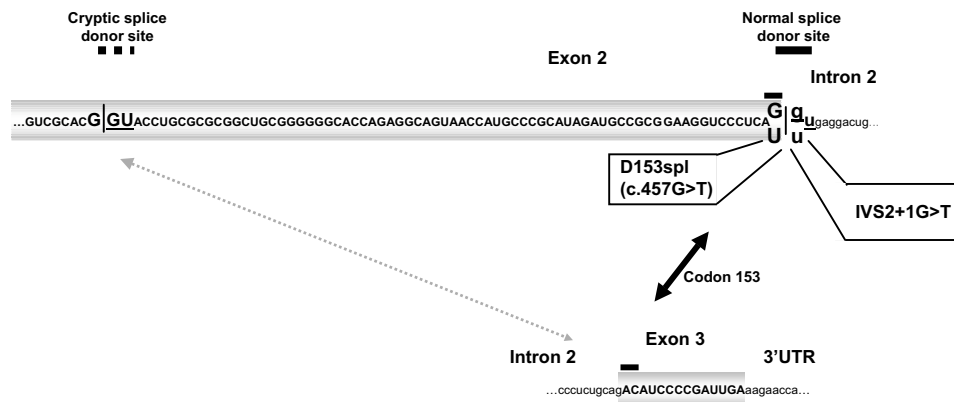


Figure 3 Schematic diagram of the cryptic splice site within exon 2 of *CDKN2A*. The partial sequence of exon 2, all of the amino acid encoding portion of exon 3 (in shaded box and in uppercase), and partial intron 2 (lower case) are shown. D153spl(c.457G>T) and IVS2 + 1G>T are indicated. The normal splice donor and acceptor sites are underlined with a solid line. The cryptic splice donor site is indicated by the dashed line and the splice site is underlined. Under normal splicing conditions, codon 153 is created with the last base of exon 2 and the first two bases of exon 3 (bar over sequence, and solid double-headed arrow). The dashed double-headed arrow indicates the splice sequence created by the mutations

splice site, indicated by the underlined nucleotides within the sequence of exon 2. The result is a frameshift from the aberrantly spliced site at amino acid R128 to the new encoded sequence (underlined): DVAR-HPRLKEPERL*.

Based on our sequence analyses of the aberrant splice products, Figure 4 shows a schematic of the four main spliced products (two for each normal transcript) resulting from the mutations at either D153spl(c.457G>T) or IVS2 + 1G>T. At the nucleotide level,

the same aberrant splice products result for both p16^{INK4a} and p14^{ARF}, but the effects on the protein coding sequences differ. For p16^{INK4a}, in the bottom half of Figure 4, the mRNA of splice product 1 α stops 74 bases short of the full-length exon 2 (indicated by the white line, Figure 4). The cryptic splice site 74 bases from the end of exon 2 splices to exon 3 and causes a frameshift. Splice product 2 α skips exon 2 entirely, creating a product that splices from exon 1 α to exon 3. The amino-acid sequence of exon 3 normally splices to the last base of exon 2 to create the aspartic acid residue, but exon 1 α remains intact with its sequence of 50 amino acids, thus causing a frameshift in exon 3. This frameshift creates an additional 39 residues before the stop codon (new sequence underlined): RPIQ-TSPIERTREALRNLGKLRSSVTEGPTGQPQLPPPQP TPLS*. (Figure 4, bottom).

The top half of Figure 4 shows the effects of the splice mutations on p14^{ARF}. Splice product 1 β does not have an effect on the amino-acid coding portion of p14^{ARF}. The stop site in exon 2 is located just upstream of the cryptic splice site (indicated by the black line in exon 2). The effect of the mutation does however delete 74 bases of the 3'-UTR. The consequence of this deletion is not known. We used the UTRScan program (Pesole *et al.*, 1999) to search the UTR functional elements for the patterns defined in the UTR site collection. We examined the 74 bases as a whole, and then examined approximately 20 bp segments separately. No obvious

3'-UTR patterns were found (not shown), but the UTRScan database is limited and the effect(s) of this deletion will need to be determined experimentally. Splice product 2 β , like splice product 2 α , skips exon 2 entirely. It forms a true p14^{ARF}/p16^{INK4a} chimera by splicing to and expressing exon 3 of p16^{INK4a}. The last four amino-acid residues for exon 1 β and the chimeric sequence of the normal reading frame of exon 3 of p16^{INK4a} is as follows: PRRP-DIPD*.

There is a possibility that there are other aberrantly spliced products in individuals with the IVS2 + 1G > T or the D153spl(c.457G > T) mutation that would be tissue specific. Material from our patients with these mutations was limited to lymphocytes. As expected, the p16^{INK4a} protein products from the lymphocytes were not detectable by Western blot analysis (not shown; Rizos *et al.*, 1997).

In summary, we have identified a mutation in the last nucleotide of exon 2, termed D153spl(c.457G > T), that results in the same splicing patterns as the previously identified IVS2 + 1G > T mutation (Hussussian *et al.*, 1994). Based on nonexperimental analysis of the genomic sequence, the initial report indicated that the IVS2 + 1G > T mutation would result in a splicing defect that caused translation through the splice site until a stop codon was reached (from DIPD* to VGD*) (Hussussian *et al.*, 1994). Our experimental data does not provide evidence for this; instead, both of these mutations reveal a cryptic splice site within exon 2 and

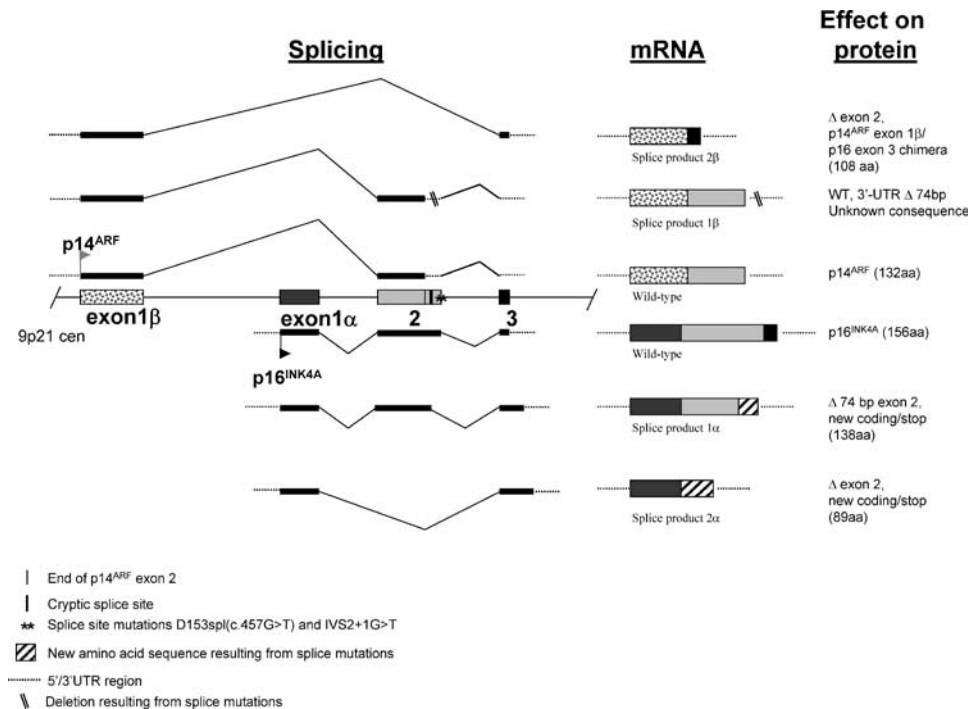


Figure 4 Diagram of normal and aberrant splicing mechanisms in lymphocytes from patients harboring a D153spl(c.457G > T) or IVS2 + 1G > T mutation. p14^{ARF}, comprising of exons 1 β and 2, is shown on the top half and p16^{INK4a}, comprising of exons 1 α , 2, and 3, is shown on the bottom half. Exons (shaded or patterned boxes) and introns (solid lines) are not drawn to scale. Angled lines indicate splicing (left panel) and dotted lines are 3'- and 5'-untranslated regions. The resulting mRNA splicing products are shown in the middle panel and the effects on the protein are explained on the right. The asterisk (*) indicates the location of the mutations and the black vertical line in exon 2 represents the end of exon 2 in ARF. The light vertical line represents the cryptic splice site (as described in Figure 3). Arrows indicate transcription start site

also cause the splicing machinery to skip exon 2 entirely (Figure 4).

It has been estimated that approximately 15% of all disease-causing point mutations result in mRNA splicing defects, with the majority (60%) of the mutations involving the GT dinucleotide at positions +1 and +2 of the splice donor site (Krawczak *et al.*, 1992). In addition to the D153spl(c.457G>T) and IVS2+1G>T mutations characterized here, a number of other splice site mutations have been described in *CDKN2A* (Hussussian *et al.*, 1994; Harland *et al.*, 2001; Petronzelli *et al.*, 2001; Lynch *et al.*, 2002). Of those molecularly characterized, the IVS1-1G>C can also cause skipping of exon 2 (Petronzelli *et al.*, 2001), while the IVS2-

105A>G mutation retains the coding sequence of exon 2 (Harland *et al.*, 2001). Further studies will be needed to examine the phenotypic consequences of these splice site mutations that affect both *CDKN2A* transcripts.

It was initially thought that mutations in exon 2 of *CDKN2A* mainly affected the p16^{INK4a} transcript and not p14^{ARF} (Quelle *et al.*, 1997; Zhang *et al.*, 1998). It has been shown, however, that exon 2 for p14^{ARF} is required for its nucleolar localization (Zhang and Xiong, 1999). Exon skipping caused by these mutations noted here would therefore disrupt this localization. Whether dual inactivation of p14^{ARF} and p16^{INK4a} leads to a lower age at onset and/or susceptibility to other cancers requires further evaluation.

References

- Goldstein AM, Struewing JP, Chidambaram A, Fraser MC and Tucker MA. (2000). *J. Natl. Cancer Inst.*, **92**, 1006–1010.
- Goldstein AM and Tucker MA. (2001). *Arch. Dermatol.*, **137**, 1493–1496.
- Haber DA. (1997). *Cell*, **91**, 555–558.
- Harland M, Mistry S, Bishop DT and Bishop JA. (2001). *Hum. Mol. Genet.*, **10**, 2679–2686.
- Hussussian CJ, Struewing JP, Goldstein AM, Higgins PA, Ally DS, Sheahan MD, Clark WJ, Tucker MA and Dracopoli NC. (1994). *Nat. Genet.*, **8**, 15–21.
- Kamb A, Gruis NA, Weaver-Feldhaus J, Liu Q, Harshman K, Tavtigian SV, Stockert E, Day III RS, Johnson BE and Skolnick MH. (1994). *Science*, **264**, 436–440.
- Kefford RF, Newton Bishop JA, Bergman W and Tucker MA. (1999). *J. Clin. Oncol.*, **17**, 3245–3251.
- Krawczak M, Reiss J and Cooper DN. (1992). *Hum Genet*, **90**, 41–54.
- Lynch HT, Brand RE, Hogg D, Deters CA, Fusaro RM, Lynch JF, Liu L, Knezetic J, Lassam NJ, Goggins M and Kern S. (2002). *Cancer*, **94**, 84–96.
- Moskaluk CA, Hruban H, Lietman A, Smyrk T, Fusaro L, Fusaro R, Lynch J, Yeo CJ, Jackson CE, Lynch HT and Kern SE. (1998). *Hum. Mutat.*, **12**, 70.
- Nobori T, Miura K, Wu DJ, Lois A, Takabayashi K and Carson DA. (1994). *Nature*, **368**, 753–756.
- Pesole G, Liuni S, Grillo G, Ippedico M, Larizza A, Makalowski W and Saccone C. (1999). *Nucleic Acids Res.*, **27**, 188–191.
- Petronzelli F, Sollima D, Coppola G, Martini-Neri ME, Neri G and Genuardi M. (2001). *Genes Chromosomes Cancer*, **31**, 398–401.
- Pomerantz J, Schreiber-Agus N, Liegeois NJ, Silverman A, Alland L, Chin L, Potes J, Chen K, Orlow I, Lee HW, Cordon-Cardo C and DePinho RA. (1998). *Cell*, **92**, 713–723.
- Quelle DE, Cheng M, Ashmun RA and Sherr CJ. (1997). *Proc. Natl. Acad. Sci. USA*, **94**, 669–673.
- Quelle DE, Zindy F, Ashmun RA and Sherr CJ. (1995). *Cell*, **83**, 993–1000.
- Rizos H, Becker TM, Holland EA, Kefford RF and Mann GJ. (1997). *Oncogene*, **15**, 515–523.
- Rocco JW and Sidransky D. (2001). *Exp. Cell Res.*, **264**, 42–55.
- Serrano M, Hannon GJ and Beach D. (1993). *Nature*, **366**, 704–707.
- Zhang S, Ramsay ES and Mock BA. (1998). *Proc. Natl. Acad. Sci. USA*, **95**, 2429–2434.
- Zhang Y and Xiong Y. (1999). *Mol. Cell*, **3**, 579–591.